Millimeter-Wave Broad-Band Fiber-Wireless System Incorporating Baseband Data Transmission over Fiber and Remote LO Delivery

Christina Lim, *Member, IEEE*, Ampalavanapillai Nirmalathas, *Member, IEEE*, Dalma Novak, *Member, IEEE*, Rod Waterhouse, *Member, IEEE*, and Gideon Yoffe

***Abstract*—We present the first demonstration of a millimeter-wave (mm-wave) broadband fiber-wireless system which incorporates baseband data transmission in both the downstream (622 Mb/s) and upstream (155 Mb/s) directions. The local oscillator (LO) required at the remote antenna base station for up- and downconversion to/from the mm-wave radio frequency (RF) is delivered remotely via a modulation scheme that is tolerant to the effects of fiber chromatic dispersion on the detected LO carrier power. The technique employs a single dual-electrode modulator located at the central office (CO) and the data and an RF signal at a frequency equal to half the LO frequency, are applied simultaneously to the device. The modulation scheme was optimized as a function of the modulator operating conditions. Simultaneous bidirectional radio transmission in the mm-wave fiber-wireless network was implemented using specially designed mm-wave diplexers located at the base station (BS) and customer unit, and a single Ka-band printed antenna array at the BS operating simultaneously in transmit and receive mode. Error-free data transmission was demonstrated for both down- (34.8 GHz) and uplinks (37.5 GHz) after 20 km of single-mode optical fiber and a bit error rate (BER) of 10^{-6} was achieved after the inclusion of a 2-m radio link.**

I. Introduction

THERE is currently great interest in the development of wireless communication systems operating at millimeter-wave (mm-wave) frequencies which are capable of providing the anticipated demand for future broad-band interactive services. The bandwidth requirements in such broadband wireless networks (up to 1 Gb/s) will demand the application of optical fiber feed networks for distribution of the radio signals to and from the remote antenna sites [1]–[4]. With regards to the technology choice for the distribution of the radio signal over fiber, several options are available including: radio frequency (RF) over fiber where the wireless signal is transported to and from the antenna base station (BS) as a mm-wave frequency [1]–[13]; intermediate frequency (IF) over fiber where lower frequency subcarriers are used to transport the radio channels with upconversion at the BS [14]–[18]; or baseband transmission where the data is upconverted to the required RF at the remote site. Millimeter-wave radio signal transmission over fiber has the advantage that the BS architecture is simplified since the requirement for mm-wave up- and downconverting mixers and local oscillators (LOs) are eliminated. In addition, the control and processing of the mm-wave wireless signals is centralized thereby allowing the central exchange to remotely monitor the mm-wave signal transmission [10]. However, fiber chromatic dispersion can have a severe effect on the achievable carrier-to-noise ratio (CNR) of the recovered radio signals in such systems [19], [20]. As a result, optical mm-wave modulation schemes which are tolerant to the effects of fiber dispersion are being actively investigated [6], [8], [21].

In contrast to mm-wave signal transmission over fiber, the effect of fiber chromatic dispersion on the distribution of lower frequency IF signals is less severe and the signals can be transported over longer fiber distances. This is also true for fiber transmission of digital baseband data signals where chromatic dispersion has a minimal effect on the delivery of subgigabits per second data streams over fiber links less than 100 km in length. In addition, both IF and baseband over fiber techniques have the advantage that they can exploit the use of mature microwave and digital hardware at the remote base station. However, the subsequent need for a mm-wave local oscillator for frequency conversion increases the complexity of the BS equipment. For mm-wave fiber-radio systems employing IF signal transmission over fiber, previous work has considered the remote delivery of the LO in order to simplify the BS architecture [16]. To date an investigation of baseband data transport schemes for application in mm-wave fiber-wireless systems has not been carried out.

In this paper, we present the first (to the best of our knowledge) experimental demonstration of a full-duplex mm-wave fiber-radio system incorporating baseband data transmission in both the down- and upstream directions. In addition, we demonstrate remote delivery of the required local oscillator for both frequency upconversion (in the radio downlink) and downconversion (radio uplink) of the data at the BS. The delivery of the LO from the central exchange or office (CO) is implemented using a novel dispersion tolerant modulation scheme whereby the LO and data signals are applied simultaneously to the one dual-electrode external modulator located at the CO. The full-duplex fiber-radio system also incorporates a broadband mm-wave printed antenna operating simultaneously

Manuscript received October 4, 1999; revised July 5, 2000.

C. Lim, A. Nirmalathas, and D. Novak are with the Australian Photonics Cooperative Research Centre, Photonics Research Laboratory, Department of Electrical and Electronic Engineering, The University of Melbourne, Parkville VIC 3052, Australia (e-mail: c.lim@ieee.org).

R. Waterhouse is with the Department of Communication and Electronic Engineering, RMIT University, Melbourne VIC 3000, Australia.

G. Yoffe is with the Australian Photonics Cooperative Research Centre, Optical Fiber Technology Centre, Sydney, Australia.

Publisher Item Identifier S 0733-8724(00)09111-8.

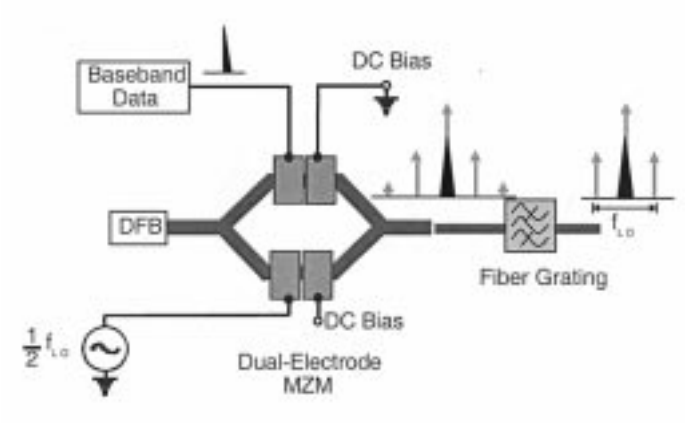

Fig. 1. Schematic diagram showing novel dispersion tolerant modulation scheme for simultaneous transport of baseband data and remotely delivered LO signal.

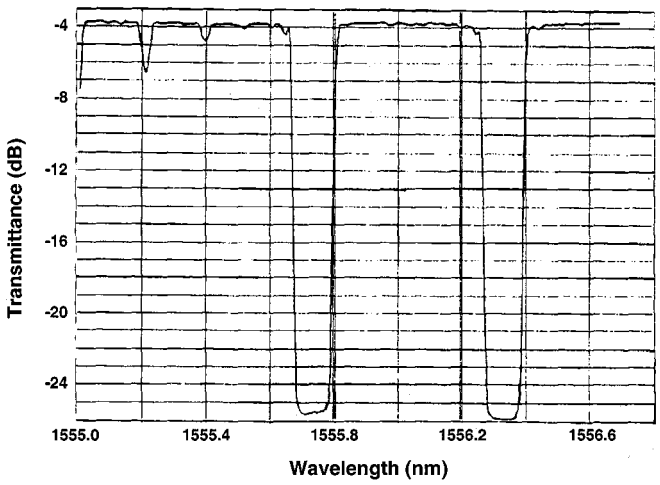

Fig. 2. Transmittance profile of the designed FG.

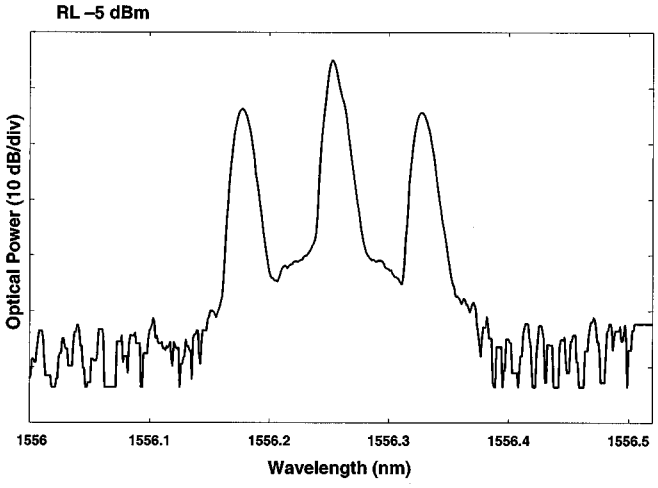

Fig. 3. Measured optical spectrum after the MZM and FG ($f_{\rm LO}/2 = 18.5$ GHz).

in both transmit and receive mode and a diplexer at the BS enabling simultaneous bidirectional radio transmission.

The paper is organized as follows. Section II provides a description of the novel modulation scheme for baseband data transmission with remote local oscillator delivery and an experimental demonstration of the technique. Section III investigates the sensitivity of the system to the modulator drive conditions in order to optimize the overall baseband data transmission system performance, while Section IV presents the demonstration of a full-duplex fiber-radio system incorporating our modulation scheme and the specially designed diplexer. Finally, conclusions are presented in Section V.

II. Modulation Scheme for Baseband Data Transmission and Remote LO Delivery

Fig. 1 shows a schematic diagram of the novel optical modulation scheme used to provide both baseband data transmission and remote delivery of the required local oscillator from the CO to the BS in a fiber-wireless system. The key features of this technique are the use of one external modulator to transmit both the baseband digital data and an analog RF signal [22], and the distribution of the LO signal in such a way that dispersion effects are minimized. In Fig. 1,the single external modulator is a dual-electrode Mach–Zehnder modulator (MZM) which is biased at quadrature and modulates the output of a distributed feedback (DFB) laser. An RF signal with frequency equal to half of the required LO frequency $(f_{\rm LO}/2)$ is then applied to one port of the MZM while the baseband data is applied to the other RF terminal. At the output of the modulator a custom-made reflective fiber grating (FG) is used to suppress second-order optical modulation sidebands spaced at $f_{\rm LO}$ from the carrier. The FG is fabricated using two gratings written in cascade in order to reflect the unwanted second-order optical modulation sidebands. Fig. 2 shows the measured transmittance profile of the FG which provides more than 20 dB rejection of the unwanted second-order sidebands relative to the optical carrier. The reflective bands with a 8 GHz bandwidth are located at approximately 37 GHz away from the optical carrier which corresponds to the designated $f_{\rm LO}$. Higher order modulation sidebands are negligible.

The optical spectrum after the FG now consists of an optical carrier modulated with baseband data and two sidebands spaced at $f_{\rm LO}/2$ from the carrier. Shown in Fig. 3 is the measured optical spectrum after the MZM biased at quadrature (4 V) and FG, with $f_{\rm LO}/2 = 18.5$ GHz, and driven by a 1557-nm DFB laser. As evident in Fig. 3, the baseband modulated optical carrier and the RF sidebands can be clearly seen. Upon detection using a high-speed photodetector, the optical carrier with the baseband modulation beats with each sideband to generate an RF signal at $f_{\rm LO}/2$ and another RF signal at $f_{\rm LO}$ is also generated resulting from the beating between the two sidebands. The recovered electrical signal will then comprise the baseband digital data and RF signals at frequencies corresponding to $f_{\rm LO}/2$ (modulated with the baseband data) and $f_{\rm LO}$.

After transmission of the optical signal over fiber to the BS, the detected RF signal at frequency $f_{\rm LO}$ can now be used as the LO for both an upconverting mixer which converts the recovered baseband data to the required wireless frequency, and a down-

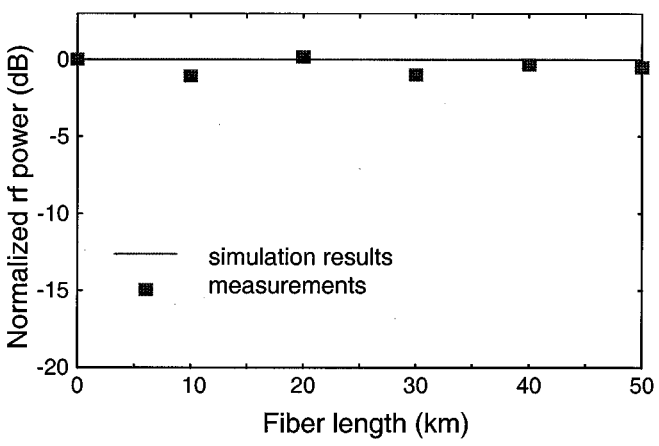

Fig. 4. Measured and predicted dispersion-induced RF power penalty for the received LO signal at 37 GHz (normalized to power at 0 km).

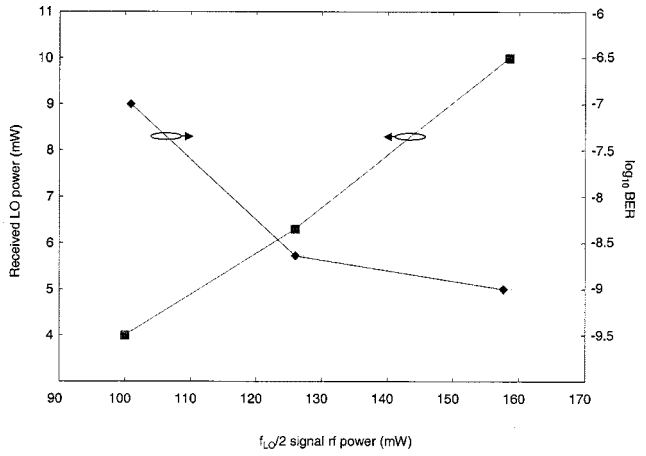

Fig. 5. Measured received LO power at BS and BER of received 622 Mb/s data at CU versus input $f_{\rm LO}/2$ signal RF power to MZM (average received optical power $= -1$ dBm).

converting mixer for the uplink mm-wave radio channel. Since the detected signal at $f_{\rm LO}$ consists of only one beat signal component (due to the two optical RF sidebands mixing with one another), transporting the LO frequency remotely in this way is highly tolerant to the effects of fiber chromatic dispersion on the detected RF carrier power [8], [19], [20]. Unlike transmission of an optical carrier with two modulated sidebands spaced at $f_{\rm LO}$, the detected signal at $f_{\rm LO}$ using the baseband modulation scheme is due to the beating between the two optical sidebands which overcomes the RF power degradation due to chromatic dispersion. This is confirmed by both measurement and theory, as shown in Fig. 4, which indicates the detected RF power of the LO signal at a frequency of 37 GHz as a function of the fiber link transmission distance. The RF power in Fig. 4 is shown normalized with respect to the detected RF power after 0 km of fiber with little variation in the detected power evident. The predicted values in Fig. 4 were obtained using a commercial photonic CAD link design platform, *GOLD*[1] with custom-designed optical and electrical circuits incorporating noise-free time-domain models. Fig. 4 shows that there is good agreement between experimental and theoretical results with the small discrepancies due to uncertainties and small variations in the dispersion parameter of the individual fiber segments (a dispersion parameter of 17 ps/nm/km was used in the simulation).

III. Performance Optimization of Baseband Modulation Scheme

The performance of the modulation scheme for simultaneous transmission of baseband data and remote delivery of a local oscillator which is tolerant to dispersion, is dependent on a number of parameters related to the operation of the dual-electrode modulator. These include the RF power of the applied signal at frequency $f_{\rm LO}/2$, the amplitudeof the input baseband data signal, and the modulator bias voltage. During the course of the experiments it was found that these variables must be carefully controlled in order to optimize the overall data transmission performance. In this section, we investigate the sensitivity of baseband data transmission using the modulation scheme described in Section II, to the MZM drive conditions.

In the downlink modulation scheme, the received optical signal is split into two paths where the baseband data and the mm-wave LO are detected separately at the BS. The received mm-wave LO signal is then used to enable up- and downconversion of the data before the radio link transmission. The conversion loss in the mm-wave up- and downconverting mixers at the BS varies as a function of the LO power, therefore the received LO signal power is critical for the optimum operation of the mixer. Since there is no automatic gain control in the BS to regulate the received LO power in our system, this parameter plays an important role in the overall system performance. In order to evaluate the performance sensitivity of the downlink, we investigate the received LO signal power as a function of the operating conditions of the MZM. In addition, we quantify the link performance by measuring the corresponding BER of the data recovered at the customer unit (CU), as a function of the modulator drive conditions.

The received LO power as a function of the applied power to the MZM RF electrode is first investigated while all other parameters are held constant. The input data amplitude was maintained at 3.2 V while the modulator was biased at the quadrature point. The RF power of the received LO signal at the BS is dependent on the optical power in the modulation sidebands generated by the MZM, which in turn is dependent on the modulator bias conditions. The difference between the optical power in the modulation sidebands and the optical carrier power reduces with increasing input RF power to the MZM. This increase in optical modulation depth will then give a larger power detected LO signal which results from the two sidebands mixing with one another. Under these conditions the received LO power also varies linearly with input RF power to the MZM, as shown in Fig. 5. The received LO power shown in Fig. 5 was measured at the input to the LO arm of the mm-wave mixer at the BS, after detection with a high-speed PD (responsivity $= 0.3$ A/W), amplification by a low noise 26.5–40 GHz amplifier with a gain of 30 dB, and followed by a 3 dB splitting loss and amplification

[1]GOLD is a product of Virtual Photonics, Inc. (www.virtualphotonics.com).

with a medium power amplifier (19 dB gain). Maximizing the received LO signal power is essential for efficient operation of the mm-wave mixers, however the maximum input RF power to the MZM is limited by the modulator electrode structure.

Fig. 5 shows the measured BER when 622 Mb/s downstream data is applied to the MZM and recovered at the CU for transmission over 0 km of fiber, as a function of the $f_{\mathrm{LO}}/2$ signal power applied to the MZM, for an average received optical power of -1 dBm. The measurement shows that the BER improves with increasing $f_{\mathrm{LO}}/2$ signal power. The eye closure at lower input RF powers to the MZM is due to the high conversion loss of the mm-wave mixer at the BS which occurs when the mixer is driven inefficiently by a relatively low received LO power. The mm-wave mixer used in our system requires a minimum of 8 dBm RF power at the LO arm for efficient operation. For this system setup, the average received optical power required to obtain a BER of 10^{-9} is -3 dBm (which includes the optical power in the modulated carrier and the two RF sidebands). This optical power corresponds to the minimum required received LO power which will efficiently drive the mm-wave mixers at the BS.

Next, we investigate the influence of modulator drift and the effect on the system performance and robustness of the link [22]. In these optimization measurements, the input $f_{\mathrm{LO}}/2$ power to the MZM and data amplitude were kept constant at 22 dBm and 3.2 V, respectively, while the bias voltage of the modulator was detuned from the quadrature point. Fig. 6(a) shows the received LO power at the BS as a function of the detuning voltage. The MZM is biased on the positive slope of the transfer function. The received LO power varies with detuned bias voltage, increasing when the MZM bias point is moved toward the MZM transfer function minimum (corresponding to a negative detuning), and decreasing when the bias voltage is increased away from quadrature toward the MZM transfer function peak (corresponding to a positive detuning). This is as expected since when the bias voltage is detuned from the quadrature point, the optical power in the MZM modulation sidebands relative to the optical carrier will vary depending on the new bias point on the nonlinear transfer function of the modulator. An increase in the received LO power indicates an increase in the modulation sideband power which in turn indicates that the MZM bias point is moving toward the minimum of the nonlinear transfer function. When the MZM bias point reaches the transfer function minimum, the modulation sidebands increase to a maximum while the optical carrier is completely suppressed, resulting in a double sideband suppressed carrier configuration. However as the MZM bias voltage varies, so does the optical carrier power and the data modulation depth, which will have a direct effect on the recovery of the modulating data and the resulting baseband data amplitude levels.

Fig. 6(b) shows the measured peak-to-peak data amplitude of the received baseband signal after detection at BS as a function of MZM bias detuning voltage. As the MZM bias point is moved closer to the modulator's transfer function maximum (positive detuning), the optical carrier power increases and the recovered data amplitude increases accordingly. In contrast, the opposite occurs as the bias voltage is tuned closer to the minimum of the modulator transfer function. The measurements in Figs. 6(a) and (b)clearly show that there exists a range of MZM bias voltages which will enable the performance of the link to be optimized.

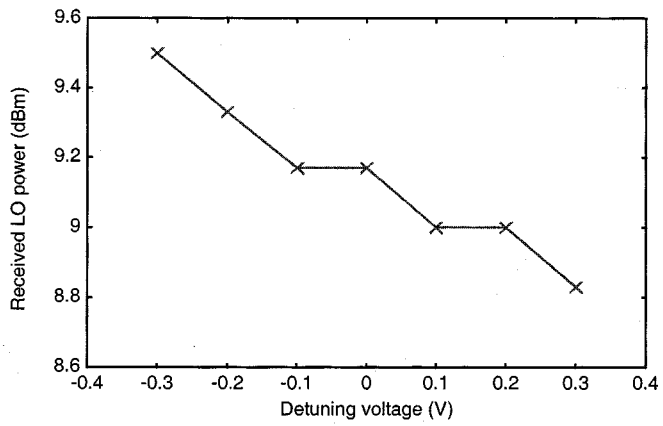

(a)

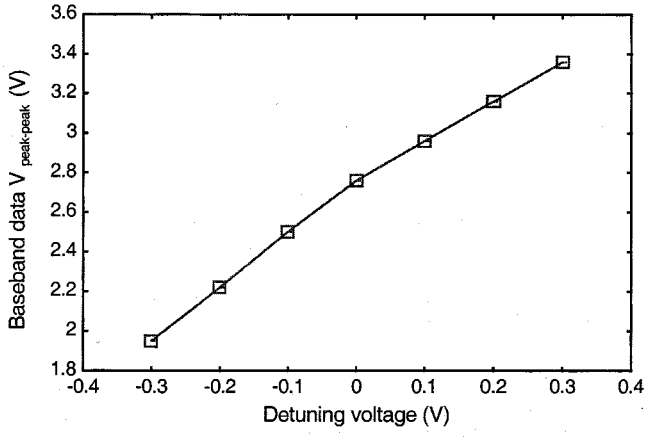

(b)

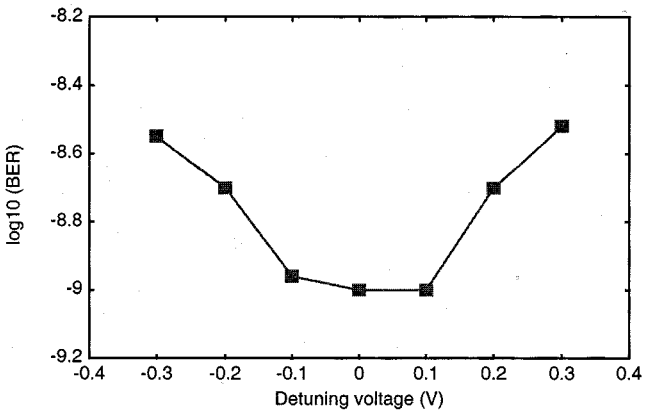

(c)

Fig. 6. (a) Measured received LO power at BS versus MZM DC bias voltage detuned from quadrature. (b) Measured peak-to-peak baseband data amplitude after recovery at BS versus MZM DC bias voltage detuned from quadrature. (c) BER measurements of recovered 622 Mb/s data at CU versus MZM DC bias voltage detuned from quadrature.

The received LO power [Fig. 6(a)] and the received baseband data amplitude [see Fig. 6(b)] at the BS determine the overall link BER. Fig. 6(c) shows the measured BER of the recovered 622 Mb/s data at the CU (for transmission over 0 km of fiber),

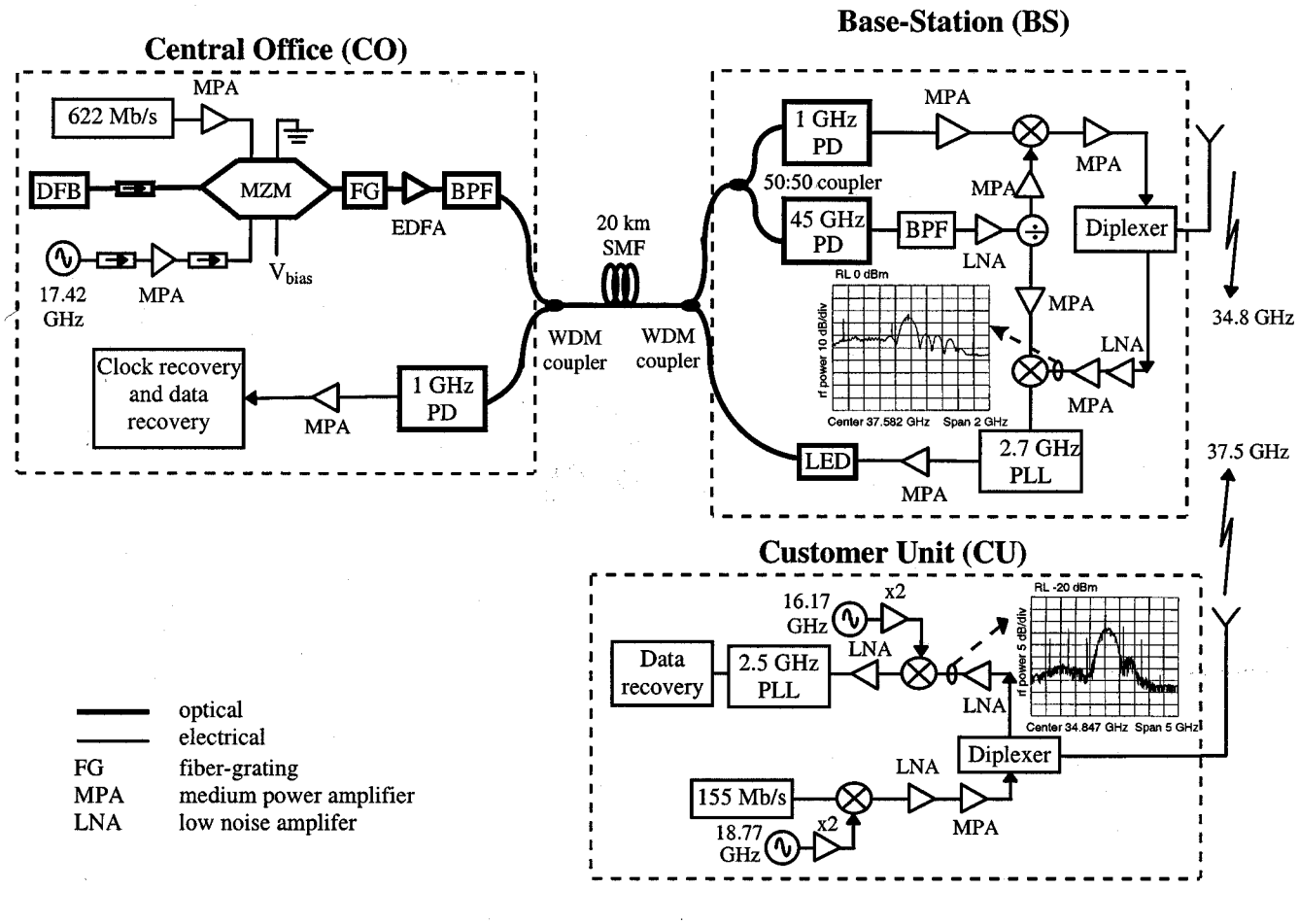

Fig. 7. Experimental setup of full-duplex broad-band fiber-wireless system with simultaneous bidirectional data transmission.

which quantifies the downlink performance as a function of the MZM bias voltage. The experimental results in this graph show that acceptable system performance (BER $\sim 10^{-9}$) can be achieved for a dc-bias variation of ± 0.1 V from the optimum bias point of the MZM at quadrature. Since it is common for the MZM dc bias voltage to drift [23], maintaining the bias voltage of the modulator reasonably close to the quadrature point via an external bias stabilization circuit [25] is important.

IV. Full-Duplex Fiber-Radio System with Baseband Data Transmission

The modulation scheme in Fig. 1 was implemented in a full-duplex mm-wave fiber-radio system incorporating baseband data transmission and the experimental setup is shown in Fig. 7. The modulation technique was located at the CO in conjunction with a 1557.0-nm DFB laser. The signals applied to the dual-electrode MZM comprised a 622 Mb/s digital data stream and a 18.5 GHz RF signal. The optical signal after the MZM is amplified using an erbium doped fiber amplifier (EDFA) and transmitted over 20 km of standard single-mode fiber (SMF) to the remote antenna BS. An optical bandpass filter (BPF) after the EDFA removes excess ASE noise. A pair of 1300/1500 nm WDM couplers were incorporated into the fiber link to allow simultaneous transmission of the down and uplink optical signals. At the BS, the optical signal is split into two paths: one followed by a 1-GHz photodetector (PD) to recover the data, and the other corporating a high-speed PD to detect the mm-wave LO signal at 34.8 GHz. The unwanted frequency component at 17.42 GHz is rejected using a mm-wave bandpass filter after the high-speed photodiode. The data and f_{LO} signals are then input into a mm-wave upconverting mixer, amplified and directed to a specially designed and fabricated

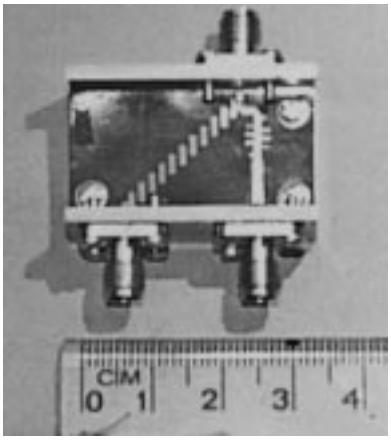

Fig. 8. Photograph of fabricated mm-wave diplexer.

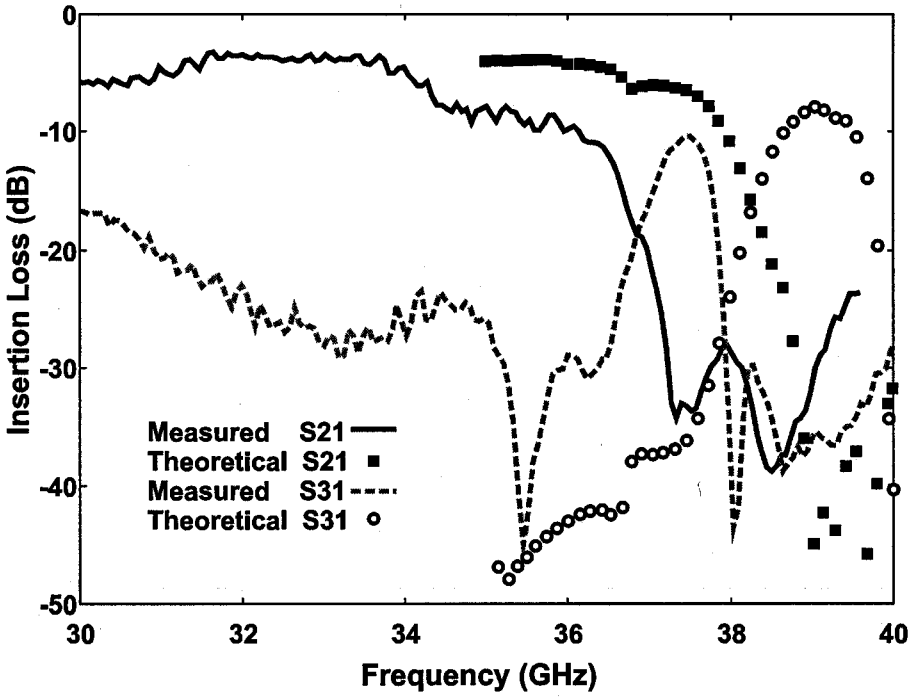

Fig. 9. Measured and calculated frequency response of the fabricated mm-wave diplexer.

mm-wave diplexer and a broadband printed antenna array to enable simultaneous bidirectional operation of the radio link. A microstrip topology was chosen for the designed diplexer and antenna in order to achieve a fully integrated and compact BS module.

The designed diplexer comprises a low pass filter for frequencies below 37 GHz (downlink) and a band-pass filter centered at 39 GHz (uplink). The low pass filter section comprises a 15-element sharp resonant filter while the high-pass section is an 11-element band-pass coupled line filter. Fig. 8 shows a photograph of the designed diplexer incorporating microstrip technology and packaged with K-connectors. Susceptance annulling was incorporated at the common input of the diplexer. The diplexer was designed using the *IE3D (Release 5)*[2] software package and etched on *Rogers RT-Duroid 5880* ($e_r = 2.2$, $d = 0.254$ mm). The theoretical and measured responses of the diplexer are shown in Fig. 9. Reasonable agreement between experiment and prediction was achieved with the expected response of the diplexer shifted down in frequency by approximately 1.5 GHz after fabrication. In addition, the insertion loss was larger than expected. These discrepancies are largely due to the fabrication errors associated with using a soft substrate at mm-wave frequencies. Since the frequency responses of the fabricated diplexer were shifted by about 1.5 GHz relative to the design carrier frequencies for the full-duplex fiber-radio system, the mm-wave RF carriers were therefore tuned to 34.8 and 37.5 GHz for the down- and upstream, respectively, in order to accommodate for the frequency shifts in the diplexer.

The transmit/receive antenna located at the antenna BS is an eight-element H-plane linear array of broad-band aperture coupled microstrip patches. The design of these patches utilized the procedure outlined in [25] to achieve the wide-band impedance response which results from the "mutual resonance" between the printed apertures and antennas. To feed the linear array of elements, a splitter consisting of seven reactive power dividers was fabricated based on microstrip technology. The measured return loss of the patch array is shown in Fig. 10 which indicates a 10-dB return loss bandwidth for the antenna of approximately 27%. Fig. 11 shows the measured H-plane radiation pattern of the eight-element linear array. As can be seen from this figure the gain of the printed antenna was approximately 15.0 dBi.

The mm-wave radio signal from the BS is radiated to a customer unit over a 2-m radio link and received using a single element broad-band printed antenna with gain of 5 dBi in conjunction with a similar mm-wave diplexer located at the CU. The signal is then amplified, and downconverted to 2.5 GHz before being passed through a phase-locked loop (PLL) circuit to recover the 622-Mb/s data stream. The inset of Fig. 7 shows the measured RF spectrum of the received signal at CU which clearly shows the data centered at the mm-wave carrier frequency of 34.8 GHz.

To demonstrate the transmission of baseband data in the upstream direction and the use of the remotely delivered LO for frequency downconversion, a 155 Mb/s, $2^{15}-1$, pseudorandom bit sequence (PRBS) at CU was used to modulate the phase of a 37.5 GHz RF carrier. This mm-wave signal is then downconverted to 2.7 GHz at the remote BS using the received LO signal delivered remotely from the CO. The modulated 2.7 GHz signal was input into a PLL to recover the 155 Mb/s baseband data which was then transported back to the CO via direct modulation of a 1300 nm light-emitting diode (LED). At the CO, the

[2]IED3 is a product of Zeland Software, Inc. (www.zeland.com).

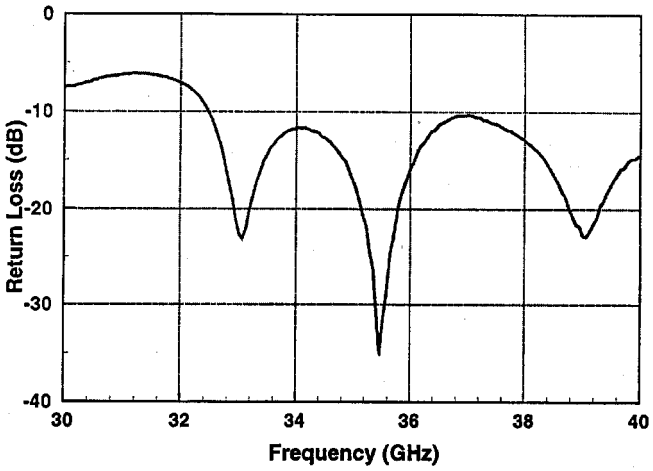

Fig. 10. Measured return loss of Ka-band eight-element linear array of aperture-coupled patches.

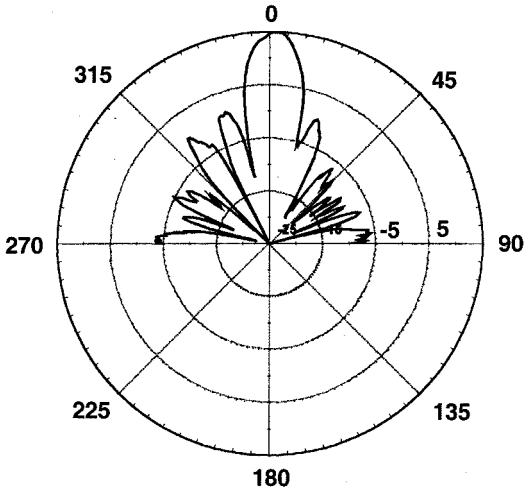

Fig. 11. Measured H-plane radiation pattern of Ka-band eight-element linear patch array.

signal was detected, amplified, and the 155 Mb/s data stream recovered using a 155-MHz clock recovery circuit.

BER measurements were carried out for the 20 km fiber link with and without the 2-m radio link and the characteristics are presented in Fig. 12. For comparison, back-to-back measurements for data transmission over 0 km of SMF without the radio link were also carried out. The measurements show that an optical power penalty $<$0.4 dB at a BER of 10^{-9} was incurred for data transmission over the 20 km fiber link. When the full-duplex radio link is included, a BER floor at $\approx 10^{-6}$ was observed for the downlink data transmission. The degradation in the BER and the presence of the BER floor is attributed to signal leakage due to the relatively poor isolation ($<$12 dB) between the different ports of the designed diplexers.

Shown in Fig. 13 are the measured BER curves of the recovered data for transmission over 20 km of optical fiber. An optical penalty of approximately 0.6 dB was observed for a BER of 10^{-9}. This penalty can be attributed to fiber dispersion due to the broad linewidth LED transmitter used at the BS. Similarly, a

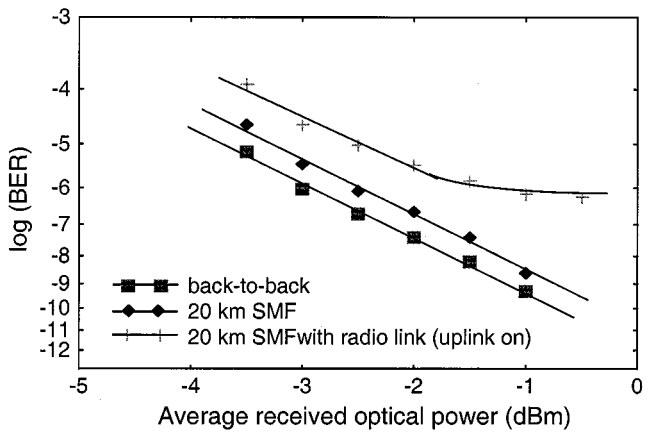

Fig. 12. BER measurements for downstream baseband 622 Mb/s data transmission in full-duplex mm-wave fiber-radio system.

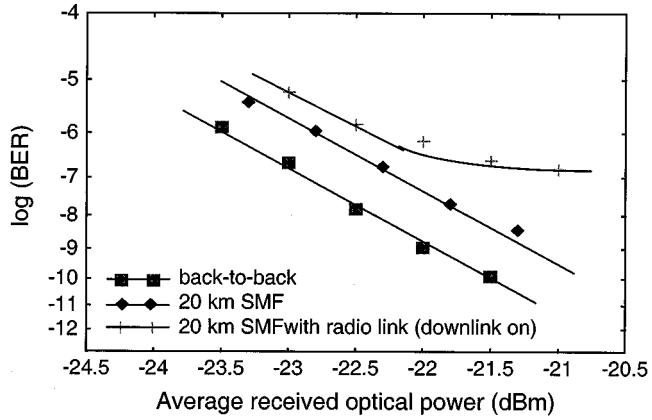

Fig. 13. BER measurements for upstream baseband 155 Mb/s data transmission in full-duplex mm-wave fiber-radio system.

BER floor at approximately 10^{-7} was seen when the radio link was incorporated for full-duplex transmission. As before, the BER floor is due to signal leakage between the diplexer ports. We envisaged that the BER for the full-duplex radio transmission can be significantly improved by incorporating diplexers with isolation $>$15 dB.

V. Conclusion

We have proposed and demonstrated a new modulation scheme for implementation in mm-wave fiber-radio systems. This technique employs baseband data transmission over optical fiber between the central office and remote antenna BS, with frequency up- and downversion at the BS achieved via remote delivery of the local oscillator from the CO. The modulation scheme employs a single dual-electrode external modulator located at the CO. Another key feature of the modulation scheme is distribution of the LO signal in such a way that the effects of fiber chromatic dispersion on the received LO power are minimized. We have also carried out a sensitivity analysis of the proposed modulation scheme in order to evaluate its tolerance to variations in the modulator drive conditions. Measurements show that the BER of the recovered

baseband data is dependent on both the received LO power at the BS, which is needed to drive the mm-wave mixers for frequency conversion, and changes in the modulator dc bias voltage. Both of these parameters must be optimized in order to achieve optimal performance of the fiber-radio system.

We have also demonstrated a full-duplex mm-wave broadband fiber-wireless system which implements our proposed modulation technique. The fiber-radio system incorporated baseband data transmission over fiber in both directions (622 Mb/s downstream and 155 Mb/s upstream) with the required local oscillator at 34.8 GHz delivered remotely. The down- and uplink radio frequencies were 34.8 and 37.5 GHz, respectively. The fiber-radio system also incorporated a specially designed Ka-band printed antenna array as the BS antenna and mm-wave diplexers for simultaneous bidirectional radio transmission. Error-free data transmission was demonstrated for both down- and upstream after transmission through 20 km of single-mode optical fiber, however due to the relatively poor isolation of the designed diplexers, full-duplex radio transmission exhibited BER floors. We believe that the BER can be improved for full-duplex radio transmission by using diplexers with >15 dB isolation.

ACKNOWLEDGMENT

The authors thank G. Smith and CSIRO Australia for assisting with the mm-wave antenna radiation pattern measurement.

REFERENCES

[1] R. Heidemann and G. Veith, "mm-wave photonics technologies for Gbit/s-wireless-local-loop," in *Proc. OECC'98*, Chiba, Japan, 1998, pp. 310–311.

[2] D. Novak, G. H. Smith, C. Lim, A. Nirmalathas, H. F. Liu, and R. B. Waterhouse, "Fiber-fed millimeter-wave wireless systems," in *Proc. OECC'98*, Chiba, Japan, 1998, pp. 306–307.

[3] U. Gliese, "Coherent fiber-optic links for transmission and signal processing in microwave and millimeter-wave systems," in *Proc. Int. Top. Meeting Micro. Photon. (MWP'98)*, Princeton, NJ, 1998, pp. 211–214.

[4] H. Ogawa, D. Polifko, and S. Banba, "Millimeter-wave fiber optics systems for personal radio communication," *IEEE Trans. Microwave Theory Tech.*, vol. 40, pp. 2285–2292, 1992.

[5] G. H. Smith, D. Novak, and C. Lim, "A millimeter-wave full-duplex fiber-radio star-tree architecture incorporating WDM and SCM," *IEEE Photon. Technol. Lett.*, vol. 10, pp. 1650–1652, 1998.

[6] C. Lim, D. Novak, and G. H. Smith, "Implementation of an upstream path in a millimeter-wave fiber-wireless system," in *Proc. Opt. Fiber Commun. Conf. (OFC'98)*, San Jose, CA, 1998, pp. 16–17.

[7] L. Noël, D. Wake, D. G. Moodie, D. D. Marcenac, L. D. Westbrook, and D. Nesset, "Novel techniques for high-capacity 60 GHz fiber-radio transmission systems," *IEEE Trans. Microwave Theory Tech.*, vol. 45, pp. 1416–1423, 1997.

[8] G. H. Smith, D. Novak, and Z. Ahmed, "Overcoming chromatic-dispersion effects in fiber-wireless systems incorporating external modulators," *IEEE Trans. Microwave Theory Tech.*, vol. 45, pp. 1410–1415, 1997.

[9] Z. Ahmed, D. Novak, and H. F. Liu, "SCM millimeter-wave (37 GHz) optical transport system for distribution of video and data signals," in *Proc. OFC'97*, Dallas, TX, 1997.

[10] J. Park and K. Y. Lau, "Millimeter-wave (39 GHz) fiber-wireless transmission of broadband multichannel compressed digital video," *Electron. Lett.*, vol. 32, pp. 474–476, 1995.

[11] D. Wake, C. R. Lima, and P. A. Davies, "Optical generation of millimeter-wave signals for fiber-radio systems using a dual-mode DFB semiconductor laser," *IEEE Trans. Microwave Theory Tech.*, vol. 43, pp. 2270–2276, 1995.

[12] Z. Ahmed, D. Novak, R. B. Waterhouse, and H. F. Liu, "Optically-fed millimeter-wave (37 GHz) transmission system incorporating a hybrid mode-locked semiconductor lase," *Electron. Lett.*, vol. 32, pp. 1790–1792, 1996.

[13] G. H. Smith, D. Novak, C. Lim, and K. Wu, "Full-duplex broadband millimeter-wave optical transport system for fiber-wireless access," *Electron. Lett.*, vol. 33, pp. 1159–1160, 1997.

[14] D. Gray, "Optimal cell deployment for LMDS systems at 28 GHz," in *Proc. Wireless Broadband Conf.*, Washington, DC, 1996.

[15] ——, "Examining the use of LMDS to enable interactive services," in *Proc. 2nd. Multimedia over Radio Congress*, UK, 1996.

[16] G. H. Smith and D. Novak, "Broadband millimeter-wave fiber-radio network incorporating remote up/downconversion," in *Proc. IEEE MTT Symp.*, Baltimore, MD, 1998, pp. 1509–1512.

[17] D. Mathoorasing, D. Tanguy, J. F. Cadiou, P. Legaud, E. Penard, S. Bouchoule, and C. Kazmierski, "Multicarrier distribution of multiple digital compressed tv channels using a harmonic laser source at 38 GHz," in *Proc. MWP'98*,, NJ, 1998, pp. 13–16.

[18] T. Kuri, K. Kitayama, and Y. Ogawa, "A novel fiber-optic millimeter-wave uplink incorporating 60 GHz-band photonic downconversion with remotely fed optical pilot tone using an electroabsoption modulator," in *Proc. MWP'98*, Princeton, NJ, 1998, pp. 17–20.

[19] H. Schmuck, "Comparison of optical millimeter-wave system concepts with regard to chromatic dispersion," *Electron. Lett.*, vol. 31, pp. 1848–1849, 1995.

[20] U. Gliese, S. Nørskov, and T. N. Nielsen, "Chromatic dispersion in fiber-optic microwave and millimeter-wave links," *IEEE Trans. Microwave Theory Tech.*, vol. 44, pp. 1716–1724, 1996.

[21] J. Park, W. V. Sorin, and K. Y. Lau, "Elimination of fiber chromatic dispersion penalty on 1550 nm millimeter-wave optical transmission," *Electron. Lett.*, vol. 33, pp. 512–513, 1997.

[22] D. J. Blumenthal, J. Laskar, R. Gaudino, S. Han, M. D. Shell, and M. D. Vaughn, "Fiber-optic links supporting baseband data and subcarrier-multiplexed control channels and the impact of MMIC photonic/microwave interfaces," *IEEE Trans. Micro. Thy. & Tech.*, vol. 45, pp. 1443–1452, 1997.

[23] C. M. Gee, G. D. Thurmond, H. Blauvelt, and H. W. Yen, "Minimizing dc drift $LiNbO_3$ waveguide devices," *Appl. Phys. Lett.*, vol. 47, pp. 211–213, 1985.

[24] S. Aisawa, H. Miyao, N. Takachio, and S. Kuwano, "DC drift compensation of $LiNbO_3$ intensity modulator using low frequency perturbation," *IEICE Trans. Commun.*, vol. E81-B, pp. 107–109, 1998.

[25] S. D. Targonski, R. B. Waterhouse, and D. M. Pozar, "Design of wideband aperture-stacked patch microstrip antennas," *IEEE Trans. Antennas Propagat.*, vol. 46, pp. 1246–1251, 1998.

Christina Lim (S'97–M'00) received the B.E (First Class Hons) and Ph.D. degrees of in electrical and electronic engineering from The University of Melbourne, Australia, in 1995 and 2000, respectively.

Since November 1999, she has been working as a Research Fellow at the Photonics Research Laboratory of the University of Melbourne in the fiber-radio group. Her research interests include fiber-optic wireless communication systems, applications of mode-locked lasers, and optical communication systems.

Ampalavanapillai Nirmalathas (M'97) received the B.E. (Hons) and Ph.D. degrees of in electrical and electronic engineering from The University of Melbourne, Australia, in 1993 and 1997, respectively.

Since 1997, he has been with the Photonics Research Laboratory (a member of the Australian Photonics Cooperative Research Centre) at the University of Melbourne, where he is now a Senior Research Fellow. His research interests include, fiber-optic feed networks for wireless systems, modeling of optical and wireless communication systems, mode-locked lasers, and microwave photonics.

Dalma Novak (S'90–M'91) received the Bachelor of Engineering (Electrical, Hons I) and Ph.D. degrees of University of Queensland, Australia, in 1987 and 1992, respectively.

In 1992, she joined the Photonics Research Laboratory (PRL) (a member of the Australian Photonics Cooperative Research Centre) in the Department of Electrical and Electronic Engineering at the University of Melbourne, where she is now an Associate Professor and Reader. She is a Key Researcher in the CRC, CRC Education Director and Deputy Director of PRL. Her research interests include fiber-wireless communication systems, semiconductor lasers and high-speed optical networks and she has published over 120 papers in these areas.

Dr. Novak is Chair of the IEEE Victorian LEOS/EDS Chapter and Chair of the IEEE Australia Council.

Rod Waterhouse (S'90–M'94) received the B.E. (Hons), M.Eng.Sc. (Research), and Ph.D. degrees from the University of Queensland, Australia, in 1987, 1990, and 1994, respectively.

In 1994, he joined the Department of Communication and Electronic Engineering at the RMIT University, where he is currently a Senior Lecturer. His research interests include printed antennas, phased arrays, optically distributed wireless systems and photonic devices for microwave applications. He has published over 120 papers in these areas. In 2000, RMIT University became a member of the Australian Photonics Cooperative Research Centre (CRC) and he is now a CRC Key Researcher.

Dr. Waterhouse is the Chair of the IEEE Victorian MTTS/APS Chapter.

Gideon Yoffe, photograph and biography not available at the time of publication.